ACID FRACTURING FEASIBILITY STUDY FOR HETEROGENEOUS CARBONATE FORMATION

A Thesis

by

ASSIYA SULEIMENOVA

Submitted to the Office of Graduate and Professional Studies of
Texas A&M University
in partial fulfillment of the requirements for the degree of

MASTER OF SCIENCE

Chair of Committee,	Ding Zhu
Committee Members,	A. Daniel Hill
	Yuefeng Sun
Head of Department,	A. Daniel Hill

May 2015

Major Subject: Petroleum Engineering

ABSTRACT

Acid fracturing is a stimulation technique that is commonly used by the industry to increase productivity or injectivity of wells in carbonate reservoirs. To determine a feasibility of acid fracturing treatment for a heterogeneous formation, the effect of rock properties on the created fracture conductivity needs to be investigated experimentally. In this study, the influence of rock lithology, porosity, and permeability on the resultant fracture conductivity was investigated for the Middle Canyon formation.

Six carbonate cores collected from different depths of Middle Canyon interval were selected for this study. The cores had the permeability ranging from 0.07 to 28 md and the porosity ranging from 1.7 to 15.4%. The acid etching experimental conditions, such as injection rate, reaction temperature, and acid type, were selected to simulate field treatment conditions. The fracture surface of each sample was scanned before and after the acid treatment to characterize the change in surface profile and to calculate the etched volume of rock.

The results of the study indicated that the final conductivity values under the maximum closure stress of 4000 psi were similar to each other (6.4 - 13.5 md-ft) for all the cores, regardless the variation in cores' porosity and permeability. It was also observed that the cores with a lower porosity had a lower decline rate of acid fracture conductivity with increasing closure stress. Based on the results of this study, it was concluded that acid fracturing stimulation of the Middle Canyon formation may not be effective to achieve the goals defined by the operator.

DEDICATION

To my parents.

ACKNOWLEDGEMENTS

I would like to thank my advisor, Dr. Zhu, and committee members, Dr. Hill and Dr. Sun for their invaluable ideas and input which increased the quality of this study.

I am specifically grateful to Dr. Zhu, Dr. Hill, and Dr. Akkutlu for their trust, understanding and support that motivated me to become a better researcher.

I also would like to thank my colleague, Xichen Wang, for showing me how to prepare the samples and run the acid etching tests, helping me with the experiments, and being a great lab partner. I am thankful to my colleague, Junjing Zhang, for his experience and help with the conductivity tests.

This thesis would not be possible without support from my family. I am thankful to my mother and father for their love, advice, and encouragement to dream big. Finally, I am grateful to Ahmet for his love, patience, humor, and unconditional support that carried me through this degree.

NOMENCLATURE

Acronyms

CO_2	carbon dioxide
EOR	enhanced oil recovery
HCl	hydrochloric acid
HCPV	hydrocarbon pore volume
OOIP	original oil in place

Variables

$N_{Re,f}$	Reynolds number for the flow along the fracture
w	fracture width, in
v	fracture flow velocity of the in the, ft/s
ρ	density, lb/ft^3 or kg/m^3
μ	viscosity, cP or Pa-s
$(p_1^2 - p_2^2)$	pressure squared difference across the fracture, psi^2
$k_f w$	fracture conductivity, md-ft
q	flow rate, liter/s
M	molecular mass, kg/kg-mol
h	height of fracture face, in
Z	compressibility factor
R	universal gas constant, J/mol-K

T	temperature, K
L	length of fracture, in

TABLE OF CONTENTS

Page

LIST OF FIGURES

Page

LIST OF TABLES

Page

CHAPTER I

INTRODUCTION AND LITERATURE REVIEW

1.1 Introduction

Acid fracturing has been widely used as an alternative to hydraulic fracturing with proppant to increase productivity or injectivity of wells in carbonate reservoirs. In acid fracturing treatments, acid is injected into the formation at a pressure above the fracturing pressure to create hydraulic fractures and open existing natural fractures. Usually, a viscous pad fluid is pumped first to initiate fracture propagation followed by injection of acid system, such as plain acid, gelled acid, cross-linked acid or emulsified acid, to create a conductive acid fracture. Hydrochloric acid (HCl) – plain or mixed with additives – is a type of acid that is the most commonly used for acid fracturing of carbonate formations. The chemical reactions of HCl with limestone and dolomite are given by

$$CaCO_3+2HCl \rightarrow CaCl_2 + CO_2 + H_2O \qquad \text{(Limestone)}$$

$$CaMg(CO_3)_2 + 4HCl \rightarrow CaCl_2 + MgCl_2 + 2CO_2 + 2H_2O \qquad \text{(Dolomite)}$$

During acid injection, several processes are taking place simultaneously. First, acid penetrates through carbonate rock down the fracture leading to fracture propagation deeper into formation. Second, acid reacts with rock at the fracture walls creating surface irregularities at fracture faces. During this process, known as differential etching, a part of the rock is dissolved by acid, creating channels with undissolved portion of the rock acting as pillars. Third, acid penetrates through formation in direction perpendicular to

fracture creating wormholes and leading to acid loss (leak to the formation). The success of acid fracturing treatment is affected by all three phenomena.

The improved well performance after a treatment is controlled by the fracture length and fracture conductivity that retains after the injection is stopped and the formation closure stress is applied on the created fracture. Acid fracture conductivity is the product of fracture permeability and fracture width that characterizes an ability of acidized fracture to create a path for fluid flow. The main parameters that determine the resultant fracture conductivity are the amount of rock removed, pattern of rock removal, and rock embedment strength. A small amount of rock dissolved at fracture face by acid results in a small fracture width and, as a consequence, in lower fracture conductivity. Likewise, a uniform etching of fracture face causes fracture walls to close under the stress due to the lack of support. Contrary, if differential etching of fracture face occurs, the created pillars would support fracture walls and leave an open channel upon fracture closure. If the rock is not strong enough to withstand the load or if a large amount of rock was dissolved by acid, the created pillars may crush under the stress, resulting in a reduced fracture conductivity.

Performance of acid fracturing treatment depends on various parameters, such as rock properties, reservoir conditions, type of acid, and treatment conditions. The primary objective of an acid fracturing design is to determine the optimum treatment conditions for a specific formation, acid type, injection rate, and acid contact time with rock.

1.2 Literature Review

In acid fracturing, the created fracture conductivity is the main parameter that determines the success of treatments. Created fracture conductivity is a function of both kinetic parameters and formation characteristics.

1.2.1 Effect of kinetic parameters on acid fracture conductivity

Kinetic parameters, such as acid type and concentration, acid contact time with formation, reaction temperature and injection rate, influence the amount of rock dissolved and the etching pattern created during acid fracturing. In one of the earliest studies on acid fracturing of carbonates (Barron et al. 1962), it was shown that the reaction rate of HCl with limestone depended on both flow velocity and fracture width. The results indicated that the reaction rate increased with increase of injection rate, while the increase of fracture width resulted in decrease of reaction rate and deeper acid penetration due to reduced shear rate.

Broaddus et al. (1968) studied the effect of acid type, temperature, and contact time on the resultant fracture conductivity. They found that acid fracturing of limestone with straight HCl at lower temperatures (80–150^{o}F) produced higher conductivity than the test with retarded acid. The results were opposite for acid fracturing performed with two types of acids at higher temperatures. Also, it was shown that the increase of contact time may improve the fracture conductivity in some cases. However, over-etching could also happen resulting in rock crushing under stress and a low fracture conductivity. The authors concluded that the maximum fracture conductivity could be achieved at the optimum etching conditions.

Anderson and Fredrickson (1989) developed a laboratory procedure to measure acid fracturing conductivity of cores in order to optimize treatment parameters. They confirmed that fracture conductivity, being affected by the amount of rock dissolved, depends on treatment parameters, such as acid type and concentration, reaction time, temperature and flow regime.

Several other researchers (Beg et al. 1998; Van Domelen 1992; Van Domelen et al. 1994) who studied the effect of contact time on the acid fracture conductivity came to the conclusion that a longer contact time did not always result in a higher fracture conductivity and the optimum contact time should be determined to achieve the maximum conductivity for a certain formation and acid type.

There have been several studies on the impact of acid type on fracture conductivity created during acid fracturing. Bartko et al. (1992) performed a number of acid fracturing experiments on limestone and dolomite cores with different acid types. The results indicated that cores acidized by 15% emulsified acid had lower conductivity than those treated by 10% emulsified acid which was attributed to greater weakening of cores by acid of higher concentration. The effect of acid retardation (reaction rate decrease) on conductivity was studied by de Rozieres (1994) for straight, gelled, and emulsified acid. The difference in conductivity for different acid system was related to diffusivity of the system. Pournik et al. (2010) compared the effect of gelled, in-situ gelled, viscolelastic, and emulsified acids on fracture conductivity. The results showed difference in conductivity for different acid systems at various closure stresses. Thus, viscoelstic acid produced the highest conductivity among all the acid systems at low

closure stress, while emulsified acid resulted in the highest conductivity at higher closure stress. For all the experiments viscoelastic acid generated the highest degree of etching among all the acid types.

1.2.2 Effect of formation characteristics on acid fracture conductivity

Although the acid fracturing kinetic parameters affect the fracture conductivity, the dominant role is attributed to formation characteristics (Anderson and Fredrickson 1989). The physical and chemical composition of the rock has a significant impact on conductivity because the etching pattern depends on degree of formation heterogeneity. Mineralogical composition will influence the reaction rate of acid with rock. For instance, calcite reacts with acid faster than dolomite. In heterogeneous formations some areas of fracture face will be dissolved to a greater extent than others resulting in differential etching. Differences in rock permeability and porosity will also influence the etching pattern due to variable acid leak-off rates (Anderson and Fredrickson 1989).

Another formation influencing the fracture conductivity is rock strength. Nierode and Kruk (1973) developed a correlation for acid fracture conductivity and found the rate of conductivity decline with increasing closure stress was a function of rock embedment strength. Anderson and Fredrickson (1989) showed that retained fracture conductivity produced by nonuniform etching would depend on the formation hardness and closure stress. The magnitude of acid fracture conductivity decrease with increasing closure stress would be affected by the formation hardness and the ratio of supporting area to etched area. Likewise, in another study on acid fracturing (Van Domelen et al. 1994) it was determined that resulting fracture conductivity is significantly influenced by

formation strength because the resistance to crushing under the stress depends on rock hardness. Abass et al. (2006) studied the effect of elastic, plastic, and creeping deformations of rock under stress on the resultant acid fracture conductivity. It was suggested that formation creeping (viscous flow) phenomenon would lead to a fast conductivity decline in a short period of time after an acid fracturing treatment. The presence of strong contact points at fracture face surface would allow to achieve greater retained conductivity under a high closure stress. Melendez (2007) performed the study of acid fracture conductivity for Texas Cream chalk, Indiana limestone, and San Andres dolomite. Among the three rock types, the Texas Cream chalk had the lowest rock embedment strength and fracture closure happened at lower stress than for limestone and dolomite. The dolomite had the highest rock strength and demonstrated the best conductivity results at high closure stress. It was also proposed that the effect of hardness variation on acid fracture conductivity was greater for dolomite than for limestone and chalk. Gomaa and Nasr-El-Din (2009) showed that in limestone formations the effect of strength reduction on fracture conductivity is greater than in dolomite formations.

1.2.3. Effect of acid leak-off on acid fracture conductivity

Fluid loss, or leak-off, takes place in acid fracturing treatments when acid penetrates into formation and wormholes are created in direction perpendicular to the fracture plane. Multiple studies on acid fracturing indicated that acid leak-off rates control the created fracture conductivity.

Beg et al. (1998) conducted a series of laboratory experiments on acid fracturing of carbonate rocks at various treatment conditions. They observed that fracture conductivity created during the test with acid leak-off was higher than conductivity in experiments, in which no fluid loss was allowed. The difference in conductivity for two experiments was greater at higher closure stress. Also, the inspection of fracture surface of the cores indicated the presence of small pits on the samples with leak-off but were absent on the samples with no leak-off. The authors concluded that acid flow into rock matrix in direction perpendicular to the fracture enhances differential etching and increases fracture conductivity.

Acid leak-off can also reduce a fracture conductivity by weakening asperities at fracture face. Gong et al. (1998) determined that a fracture conductivity decreases as both leak-off rate and contact time increase. Pournik et al. (2010) performed the analysis of both leaked-off acid and spent fracture flow acid by measuring calcium content and acid concentration. The results showed that acid leak-off played the major role in fracture etching with minimal contribution from acid flow along the fracture.

1.3 Research Objectives

The current research aims to evaluate the acid fracturing efficiency of heterogeneous carbonate formation through experimental study on core samples of different lithology, porosity, and permeability.

There are two main objectives for this study:

1. Understanding the effect of rock properties, such as lithology, porosity and permeability, on the acid etching behavior and the created fracture conductivity.

2. Determining the feasibility of acid fracturing treatment for Middle Canyon formation of SACROC Unit and identifying the optimum conditions for the treatment.

CHAPTER II

EXPERIMENTAL APPARATUS AND PROCEDURES

2.1 Experimental Apparatus

In this study, an experimental set-up containing the acid fracture conductivity cell was used to perform the acid etching of core samples. The test cell was a modified API RP-61 conductivity cell made of Hastelloy C-276 corrosion resistant material. The experimental apparatus used in this study allows an appropriate scaling of acid fracturing treatment to represent field conductions. The core samples selected for this study had a rectangular shape with rounded ends and the dimensions of 7.25 inches in length, 1.75 inches in width, and 3 inches in height to provide a perfect fit of a sample inside the cell. The sample is mounted into the cell leaving a gap of 0.12 inches between two halves of the sample to represent a fracture. The cell is place vertically to avoid gravity effects during acid injection. The sample is sealed inside the cell by inserting two side pistons. The main flow stream along the fracture is introduced through the fittings in the flow inserts at the bottom and top of the cell. Leak-off is allowed by providing a flow path through the cores in direction perpendicular to the main flow and then through the channels in the side pistons. Leak-off is controlled by adjusting back pressure. The schematic diagram of acid fracturing apparatus is shown in **Figure 1**.

The fluid is pumped into the cell by a piston pump from either the water tank or the acid tank. The maximum injection capacity of the pump used is 1 liter/min. The cell was heated up by a heating jacket during the experiments to simulate the field conditions

when acid of ambient temperature is injected into formation of elevated temperature. The cell was pressurized by nitrogen gas to keep the pressure at 1000 psi. This allowed to maintain CO2 gas – a product of a chemical reaction between carbonate and HCl – in solution. The cell pressure and leak-off pressure were monitored by pressure transducers connected to the cell midpoint pressure port and to the side pistons' pressure ports.

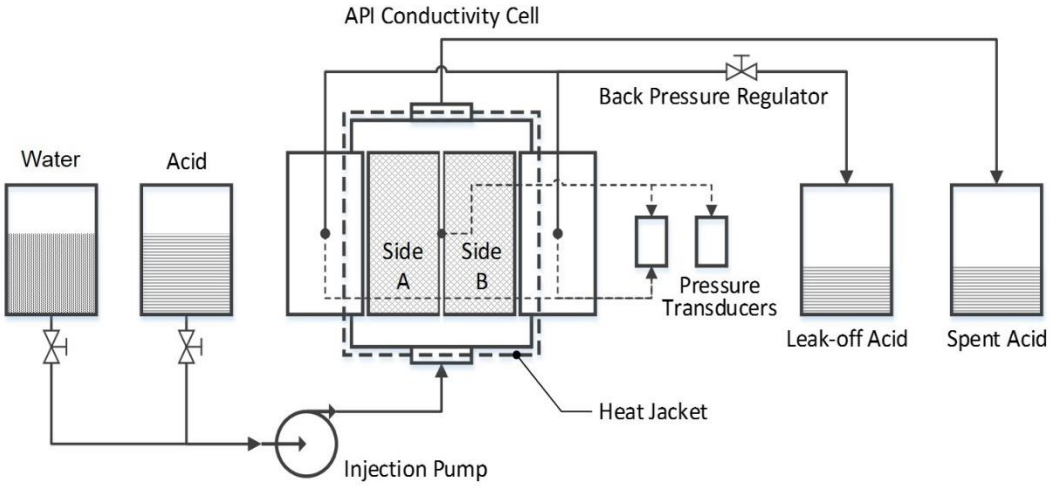

Figure 1. Acid etching apparatus diagram

The acid fracture conductivity was measured using the apparatus shown in **Figure 2**. The conductivity set-up consisted of two main elements – the modified API conductivity cell and the load frame. The conductivity cell has the same dimensions as the acid etching test cell and is made of stainless steel. The core samples are mounted into the cell and sealed with the top and bottom pistons. The flow inserts are connected to the sides of the cell to allow the flow of nitrogen gas through the cell. The inlet line is connected to the nitrogen tank with a pressure regulator which is used to set the cell

pressure. The outlet line is equipped with a backpressure regulator that allows controlling the flow rate. The cell is placed horizontally on the load frame and the closure stress is applied at an increment of 100 psi per minute on the top piston which is in contact with the core sample. Cell pressure and differential pressure across the fracture are measured with the pressure transducers which are connected to the data acquisition system and the computer. For each closure stress pressures are measured at four different flow rates, and the Darcy's law for gas flow is used to calculate the fracture conductivity base on four data points.

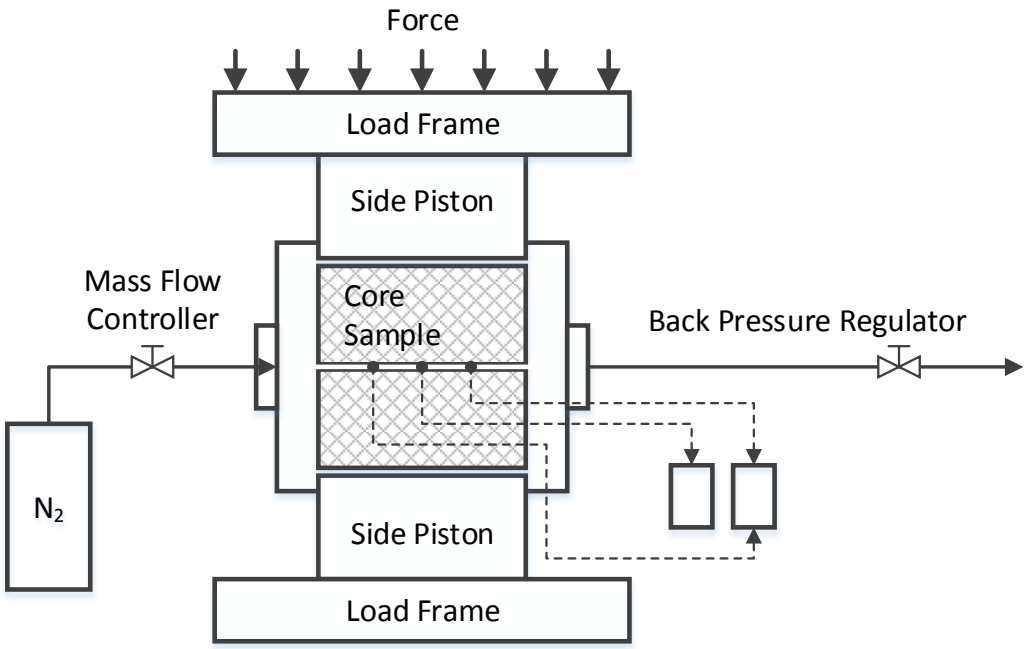

Figure 2. Fracture conductivity apparatus diagram

2.2 Core Samples Preparation

The first step of the experiment is to prepare core samples. Six carbonate cores were selected for the study. Cylindrical cores were cut to the shape of rectangular blocks of 5.4 inches length, 1.7 inches width, and 3 inches height. Each sample was cut in half to have two pieces of 5.4 inches by 1.7 inches by 1.5 inches. The sample needs to be 7 inches long, 1.7 inches wide, and 6 inches tall to fit the test cell. To make up for the required sample size the sandstone blocks with rounded edges were glued to the sides of the carbonate cores (**Figure 3**).

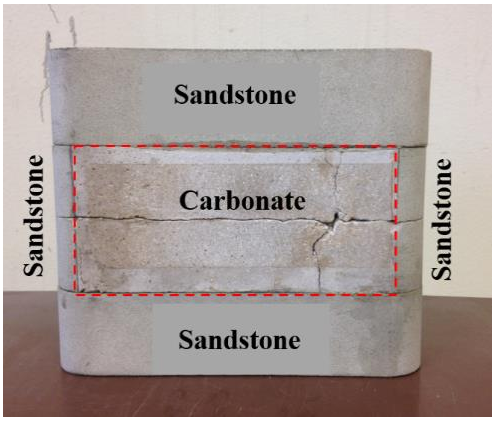

Figure 3. Core sample for an API modified test cell

Sample cores were then coated with silicone-based sealant to provide a perfect fit of a sample inside the test cell. The following steps describe this process in detail:

1. Tape two halves of the core sample with white tape to protect from silicone entering the fracture.
2. Tape the top and the bottom of the sample with blue tape to protect the cores from silicone contamination.

3. Apply three layers of the silicone primer on to the sample allowing 15 minutes drying time between each application.
4. Clean metal surface of the mold with acetone and apply two layers of silicone release spray. Wait for 3 minutes between applications.
5. Assemble the mold and position the sample inside the mold. The sample is prepared in three stages (**Figure 4**). For the first stage attach the plastic and metal plates to the bottom of the mold before placing the sample inside.

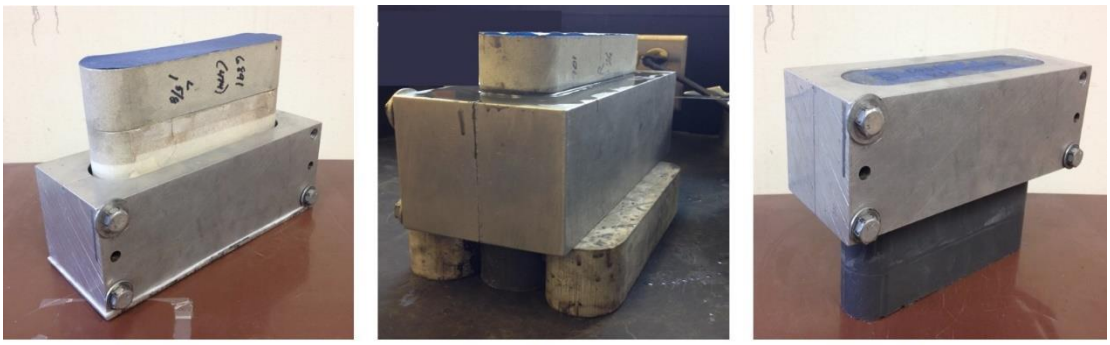

Figure 4. Core sample preparation in 3 stages

6. Mix silicone potting compound with silicon curing agent in the ratio of 1:1 by weight and stir the mixture well to obtain a homogeneous grey-colored liquid.
7. Pour the mixture into the gap between the mold and the sample.
8. Leave the sample for 1 hour at room temperature.
9. Put the mold with the sample into the oven and set the temperature to 60°C. Bake the sample inside the oven for 3 hours.
10. Remove the sample from the oven and let it cool down for 10 minutes.

11. Disassemble the mold and extract the core sample.
12. Cut the silicone at the edges with a razor to make a smooth surface for the next stage.
13. Repeat all the steps for the second and the third stages. In step 5, do not use the bottom of the mold for sample preparation. For the second stage, place the mold in the middle of the core sample so that the lower edge of the mold covers about 0.4 in of the silicone coating from the first stage. For the third stage, place the mold on the top of the sample.

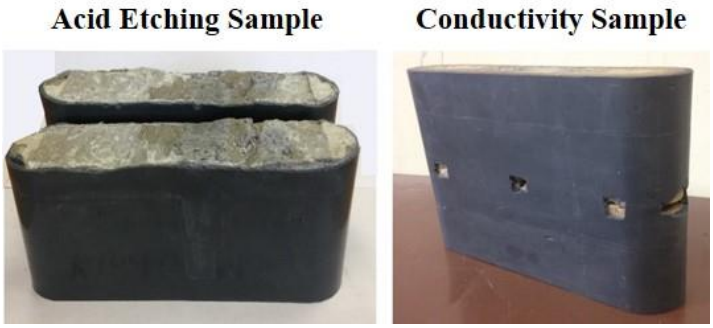

Figure 5. Core samples final view before etching test and conductivity test

14. After the sample preparation is complete, for acid etching experiment, cut the silicone in the middle of the sample along the fracture and separate two halves of the sample (**Figure 5, left**). For the conductivity experiment, cut the windows in silicone coating on the front side of the sample to ensure pressure communication between the fracture and the transducers. Also, cut the windows on the sides of the sample to allow gas flow through the fracture during the experiment (**Figure 5, right**).

2.3 Acid Etching Experimental Procedures

Acid etching experiment was done by following the procedures below.

1. Saturate the core samples with water by using the glass vessel with a lid connected to the vacuum pump. The gauge in the vessel lid should indicate around -13 psi during saturation process.
2. Remove the cores and dry them with a paper towel. Wrap one layer of teflon tape around the cores and apply a thin layer of vacuum grease on the sides of the cores.
3. Place the test cell in a vertical position on the frame and insert the cores into the cell by using the hydraulic jack. The cores should be placed in a vertical position inside the cell in such a way that the flow direction is set upwards and the gap of about 0.12 inches is left between the cores.
4. Insert the pistons into the cell and push them inside using the hydraulic jack until they touch the core samples.
5. Assemble the flow inserts and connect all the lines. Make sure that the hydraulic jack is locked to prevent movement during acid injection.
6. Place the outlet line's end into the sink, open the valve on the water supply line to the pump and start the pump.
7. Set the cell pressure to 1000 psi and the leak-off differential pressure to 20 psi. Set the injection rate to the required value.
8. To ensure that laboratory experiment represents field treatment, the Reynolds number for the flow along the fracture needs to match for both field and laboratory conditions. The Reynolds number for the flow along the fracture is defined as:

$$N_{Re,f} = \frac{wv\rho}{\mu} \qquad (1)$$

where w is fracture width, v is mean velocity of the flow in the fracture, ρ is fluid density, and μ is fluid viscosity.

9. Using the field treatment conditions with the injection rate of 30 bbl/min and the typical fracture dimensions (100 ft long and 0.2 in wide), the injection rate during the experiment should be 3.4 L/min. As the acid moves along the fracture and leak-off occurs, the flow velocity and the Reynolds number decrease. The injection rate of 1.1 L/min was used in the experiment which corresponds to the maximum injection capacity of the pump.
10. Wrap a heating jacket around the cell, set the temperature to 125°F, and start the heating process.
11. Pour 11 liters of the gelled acid into an acid mixing tank. The fluid contains 15% HCL premixed with Ultra Gel 950 gelling agent.
12. After the desired temperature is achieved, switch the injection fluid from water to acid by closing water line valve and opening acid line valve at the same time. Make sure to place the outlet line into an acid disposal barrel before switching the fluids.
13. Start acid injection and monitor the process for the desired contact time. In our case 10 minutes contact time was used.
15. After the acid etching is completed, change the flow from acid to water. Turn off the heating jacket and keep flushing the system with water until the universal indicator paper shows neutral pH of the liquid from the outlet.
16. Depressurize the system, turn off the pump, and close the water line valve.
17. Disassemble the cell and push out the core samples with the hydraulic jack.

18. Clean the cell and flush the lines with air.

2.4 Conductivity Measurement Experimental Procedures

Conductivity measurement was performed by following the procedures below:

1. Remove the silicone coating from the core samples after the acid etching test and re-prepare the samples following the procedure described in Section 2.1.
2. Cut the windows in the silicone coating for gas flow inlet/outlet and for pressure transducers.
3. Wrap 4 layers of teflon tape around the core samples on the top, in the middle, and at the bottom of the sample. Apply silicone grease on the sides of the cores.
4. Insert the core sample into the conductivity cell using the hydraulic jack.
5. Insert the side pistons into the cell to prevent the movement of the cores once closure stress is applied by the load frame.
6. Place the conductivity cell in a horizontal position in the center of the load frame to ensure an even distribution of the force on the contact area. Align the flow direction with the corresponding inlet.
7. Connect the flow inserts and the lines. Make sure the inlet valve is open and the back pressure regulator is closed.
8. Lower the piston of the load frame until it touches the top piston of the cell.
9. Open the nitrogen tank and pressurize the cell to 50 psi. If the pressure does not build up, it may indicate a leak in the system. In this case disassemble the cell and repeat the procedure.
10. Apply 500 psi closure stress and let the cell pressure stabilize for 30 minutes.

11. Open the back pressure regulator and set the first flow rate. Record the cell pressure and the pressure drop across the fracture after stabilization.
12. Repeat the readings for 4 different flow rates. Keep the cell pressure at 50 psi for each flow rate by adjusting the backpressure regulator.
13. Increase the closure stress from 500 to 4000 psi in 500 psi steps and repeat the measurements for each closure stress.
14. Turn off the nitrogen flow and lift the load frame piston to release the stress and to allow the removal of the conductivity cell.
15. Disconnect the flow lines, disassemble the cell, and remove the cores using the hydraulic jack.

To calculate the conductivity, the Darcy's law for gas flow in porous media was used:

$$\frac{(p_1^2 - p_2^2)M}{2ZRTL} = \frac{1}{k_f w}\frac{q\rho\mu}{h} \qquad (2)$$

Equation 2 is in a form of straight line where the slope corresponds to the inverse of conductivity. The pressure squared difference, $(p_1^2 - p_2^2)$ and the flow rate, q are measured during the experiment under different closure stresses. The values for all the other variables are given in **Table 1**.

Table 1. Parameters used for conductivity calculation

M	Molecular mass of nitrogen, kg/kg-mol	0.028
h	Height of fracture face, in	1.65
Z	Compressibility factor	1.00
R	Universal constant, J/mol·K	8.3144
T	Temperature, K	293.15
L	Length of fracture over which pressure drop is measured, in	5.25
μ	Viscosity of nitrogen at standard conditions, Pa·s	1.7592×10^{-5}
ρ	Density of nitrogen at standard conditions, kg/m^3	1.16085

2.5 Fracture Face Surface Characterization

The profilometer apparatus (**Figure 6**) was used to characterize the fracture face of the core sample. This device uses a laser displacement sensor that measures the surface topography variation in vertical direction (z coordinate) as a function of position on the surface (x and y coordinates). The sample is being moved along its length (in x direction) on a moving table and the measurements are being taken. Then, the sample is moved 0.05 in along its width (in y direction) and the measurements are taken along the sample length. The process is repeated until the entire surface area is covered. The profilometer allows measuring the change in fracture face topography after acid etching and to calculate the total volume of the rock dissolved. To do this, the surface of fracture face of each sample was scanned before and after acid etching experiment. During scanning the direction of laser displacement was the same as the direction of the flow during the acid etching experiment.

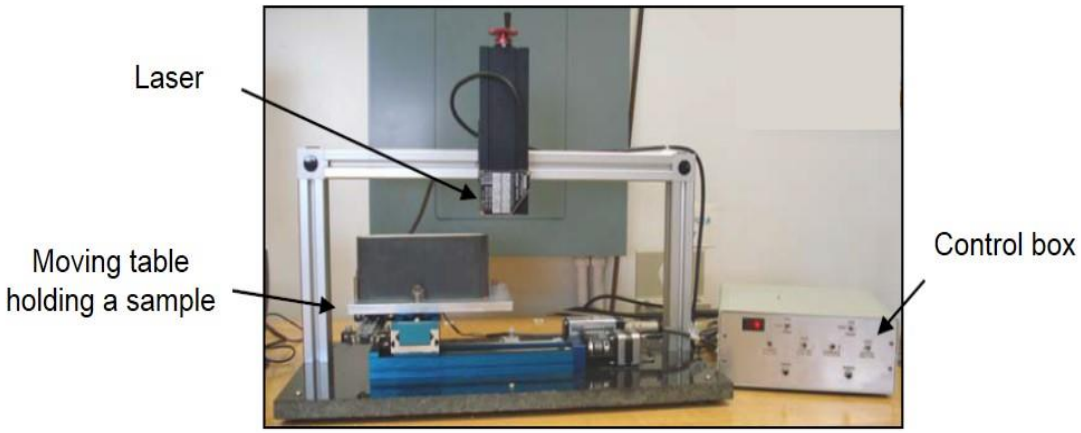

Figure 6. Profilometer device for fracture face surface characterization

CHAPTER III

EXPERIMENTAL RESULTS AND DISCUSSION

3.1 Case Study Background

The SACROC Unit is the largest operating unit in the Horseshoe Atoll carbonate platform which was formed during Permian in the Midland Basin (**Figure 7**). It is bounded by the Diamond M Field to the south and separated by a narrow channel from the Cogdell Field to the north. SACROC is composed of Cisco and Canyon formations at an average depth of 6700 feet and covers the area of 50,000 acres.

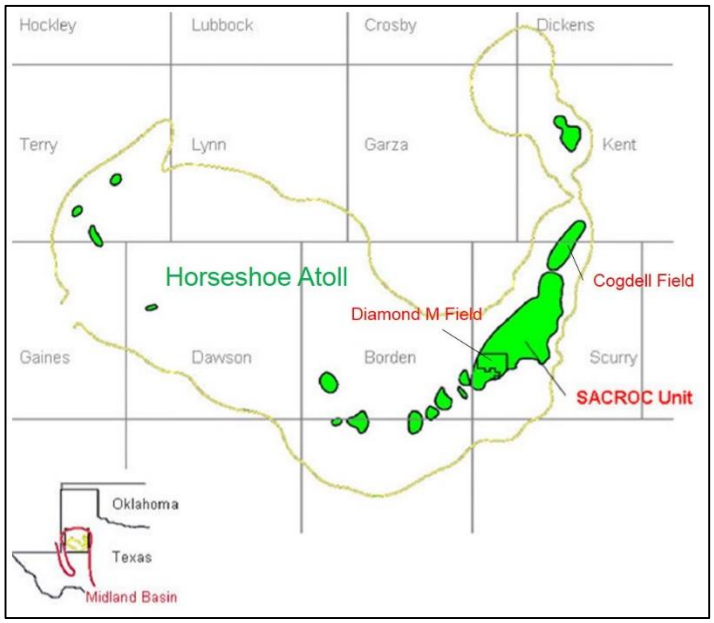

Figure 7. SACROC unit location map

The reservoir includes three pay zones – Cisco, Green Zone and Middle Canyon, which is further subdivided into Upper Middle Canyon and Lower Middle Canyon units

(**Figure 8**). The reservoir is highly heterogeneous, both vertically and horizontally, and has an average porosity of 0.076 and an average permeability of 19 md. The reservoir quality is decreasing from Green Zone, followed by Upper Middle Canyon (UMCN) and Cisco intervals. Lower Middle Canyon (LMCN) have the lowest porosity and permeability across the Unit. Both Cisco and Green Zone intervals contain vugs and highly permeable natural fractures that act as thief zones during fluid injection.
The development of the Unit began from discovery of Kelly Snyder Field in 1948 with an estimated OOIP of 2.8 billion barrels. After the reservoir pressure dropped from 3,122 psi to 1800 psi, the waterflooding was started in 1954 to increase the production. In 1974, CO_2 injection was started in addition to waterflooding. CO_2 was injected alternatively with water (WAG) in relatively small percent HCPV.

In the mid-1990s it was decided that the existing EOR technique does not allow to effectively recover oil, and three CO_2 flooding projects were initiated in the northern, central and south-western parts of the unit. Positive oil production response to redeveloped CO_2 injection has leaded to a further expansion of the project.

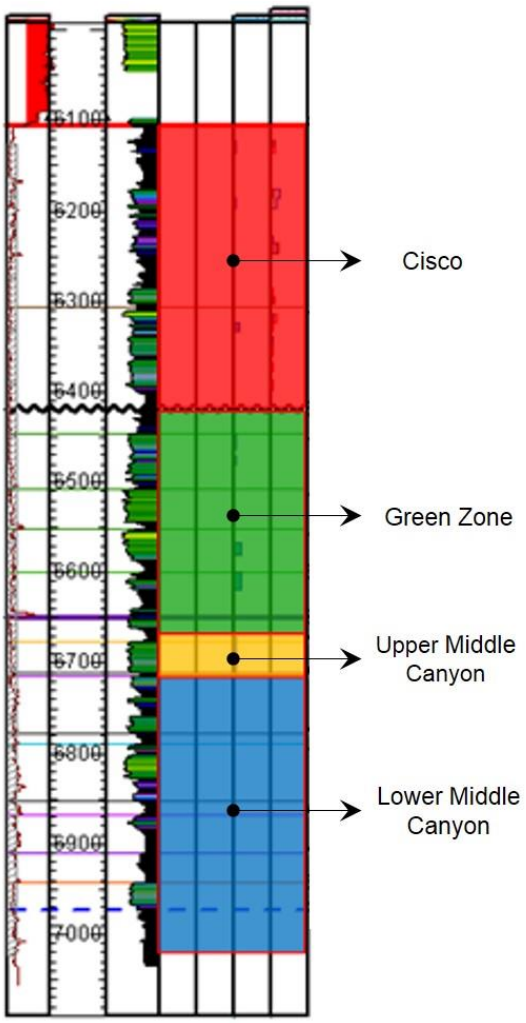

Figure 8. SACROC unit pay zones

3.2 Problem Description

The current stage of CO_2 injection EOR project uses injection wells with horizontal laterals of 4000-5000 ft long drilled in Middle Canyon interval. As was mentioned earlier, this carbonate formation is characterized by low porosity and consists of heterogeneous layers with permeability ranging from almost zero to 30 md. To increase the injectivity of the wells drilled in the low permeability zone, it has been

decided to perform a multistage acid fracturing stimulation. The created acid fractures need to be highly conductive to achieve required CO_2 injection rates and relatively short in order to prevent short circuit of CO_2 directly from injection to production wells through highly permeable regions of Green Zone interval.

The acid fracturing performance depends on both treatment conditions and formation properties. In order to design an optimum acid fracturing treatment of a heterogeneous formation, such as Middle Canyon, the influence of rock lithology, porosity and permeability on the resultant fracture conductivity needs to be understood.

3.3 Samples Description

Six carbonate cores were selected for this study to evaluate the feasibility of acid fracturing of heterogeneous formation. The values of porosity and permeability, as well as the lithology of the core samples, have been previously defined by the company that provided the cores for this study. The **Table 2** summarizes the properties of the cores. All the cores were collected from different depths of Middle Canyon formation. The selected cores have the permeability ranging from 0.07 to 28 md and the porosity varying from 1.7 to 15.4%.

Table 2. Rock properties of the tested core samples

Sample	Depth, ft	Perm, md	Poro, %	Lithology
KM 6831	6,831	28.00	8.4	Mud-dominated packstone
KM 6847	6,847	3.60	14.0	Mud-dominated packstone
KM 6878	6,878	0.07	1.7	Limestone dense silty laminated
KM 6891	6,891	0.54	9.0	Dolomite and Limestone slightly sandy slightly silty scattered pin-point porosity fossiliferous silty laminated
KM 6898	6,898	8.20	15.4	Grain-dominated packstone
KM 6901	6,901	3.26	12.9	Dolomite and Limestone slightly sandy slightly silty scattered pin-point porosity fossiliferous

For the purpose of comparison, the porosity and permeability data for the cores were plotted as the clustered column charts with a Cartesian scale for the porosity values axis and a logarithmic scale for the permeability values axis (**Figure 9** and **Figure 10**).

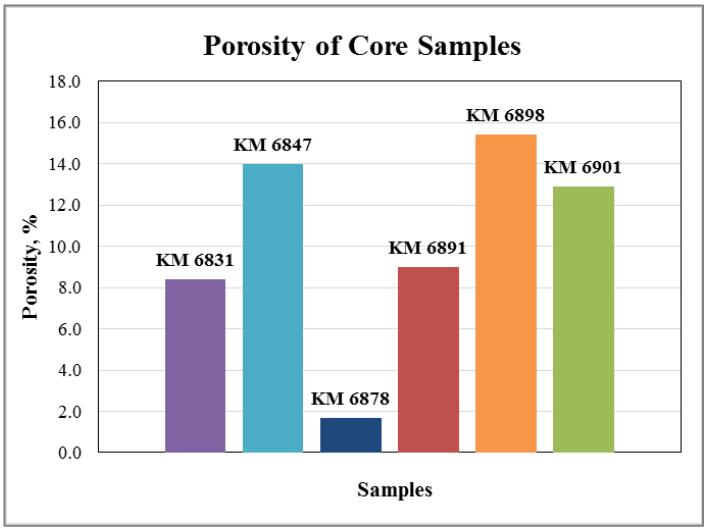

Figure 9. Porosity of the tested core samples

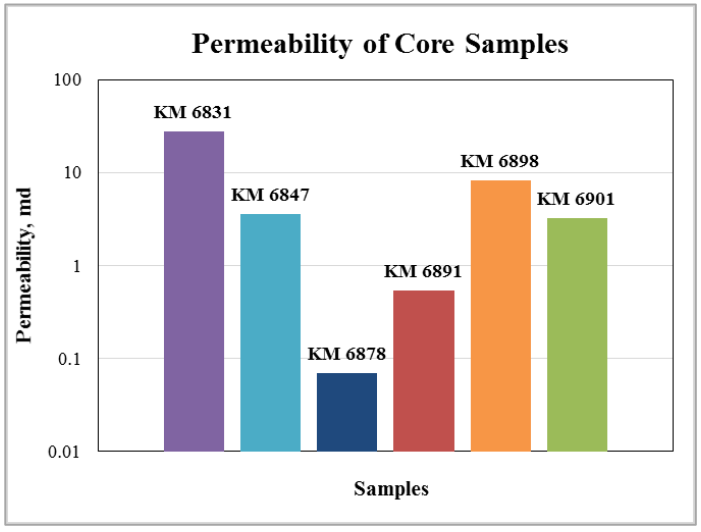

Figure 10. Permeability of the tested core samples

3.4 Acid Etching Results

Six acid etching experiments were performed on the selected carbonate cores. During each of the experiment the parameters, such as cell pressure (1000 psi), cell temperature (125^{o}F), and the type of the acid system used (15% HCl mixed with Ultra Gel 950 gelling agent) were kept the same. The contact time, the acid injection rate, and the leak-off were different only for the first experiment, while these parameters were identical for the rest of the tests.

The first experiment was conducted with the core sample KM 6878. The contact time for this experiment was 10 minutes and the injection rate was set to 1 liter/min to properly scale the laboratory test to the field conditions. No acid leak-off was allowed throughout the test. After the acid etching experiment the amount of total etched volume of the rock at fracture face was calculated to 0.127 in^3, which was about four times lower than a typical value of the rock volume dissolved during acid etching of carbonate cores (Melendez 2007). After visual inspection of the sample KM 6878, it can be seen that the core consists of layers of darker and lighter rock elongated in direction perpendicular to the fracture length and the acid flow. Also, this sample has the lowest porosity and permeability. All these factors may be the reason for such a small amount of rock etched at the fracture surface during the acid treatment. The 3D image of the fracture surface profile shown in **Figure 11** indicated a low degree of etching during the acid treatment of this core. The acid fracture conductivity results for this core reported in the next section confirmed that an insufficient conductivity was created at the experimental conditions used for the acid etching test. Thus, it was decided to increase the acid contact time from

10 minutes to 20 minutes and to allow the leak-off for the rest of the experiments. Due to the limited amount of acid, the injection rate was decreased two times to maintain the total injected volume of acid the same as for the first experiment (10 liters). The contact time, leak-off volume and total etched volume for all of the experiments are summarized in **Table 3**.

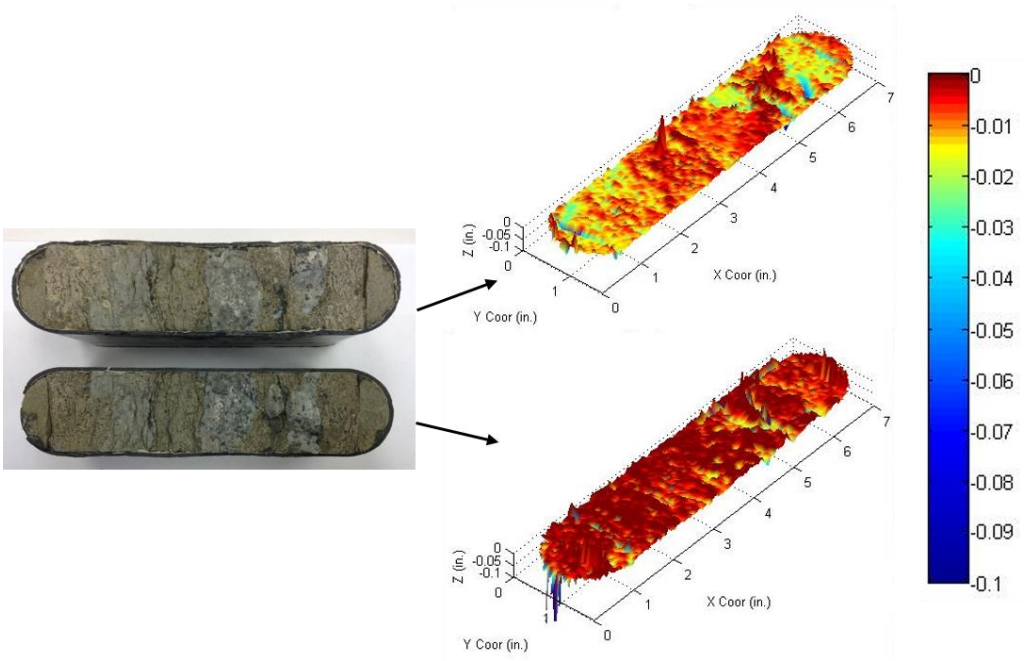

Figure 11. Difference in surface profile created by acid etching of core KM 6878

Table 3. Summary of acid etching experimental conditions and results

Sample	Contact time, min	Leak-off Volume, ml	Total Etched Volume, in^3
KM 6878	10	No leak-off	0.127
KM 6831	20	2,633	1.037
KM 6847	20	387	0.460
KM 6891	20	2,046	0.477
KM 6898	20	536	0.952
KM 6901	20	448	0.484

The leak-off volumes for two of the samples, KM 6831 and KM 6891, were significantly higher than for the other cores, with KM 6831 being the highest one. The reason for this phenomena can be explained as both of the samples had fractures created during cores cutting. The created fractures could act as easy paths for acid to penetrate through the cores perpendicular to the flow along the fracture. In addition, the core KM 6931 has the highest permeability among all the cores which would increase the leak-off during acid etching test. Also, KM 6831 sample had a rough fracture surface, while the rest of the cores had much smoother fracture surface, which indicates that mineralogy and mechanical properties of KM 6831 are different from other cores. Interestingly, the core KM 6901 has the natural fracture in the middle of the core, however, the leak-off volume for this sample was not as high as for the other two cores discussed above and was comparable to the leak-off volumes for the cores without fractures. This may be related to the depth and the geometry of the fracture.

The etched volumes for the experiments with contact time of 20 minutes were about 0.47 in^3 for the cores KM 6847, KM 6891 and KM 6901, and about 1.0 in^3 for the cores KM 6831 and KM 6898. It was observed that the total etched volume of the rock correlated with cores' permeability values. The core samples KM 6831 and KM 6898 that had the greatest amount of rock dissolved during acid etching, had the highest permeability values among all the samples, 28 md and 8.2 md respectively. The cores with the total etched volume of rock of about 0.47 in^3 had the permeabilities ranging between 0.54 and 3.6 md. The core sample KM 6878 had the lowest permeability (0.07 md) and the minimum total etched volume (0.127 in^3). The relationship between

total etched volume and permeability was found to be exponential with $R^2 = 0.081$ (**Figure 12**). No correlation was found between the total etched volume and the porosity for the acid etching experiments of the core samples. Thus, the amount of rock dissolved during etching and the pattern of rock removal are more likely to be governed by rock permeability rather than porosity.

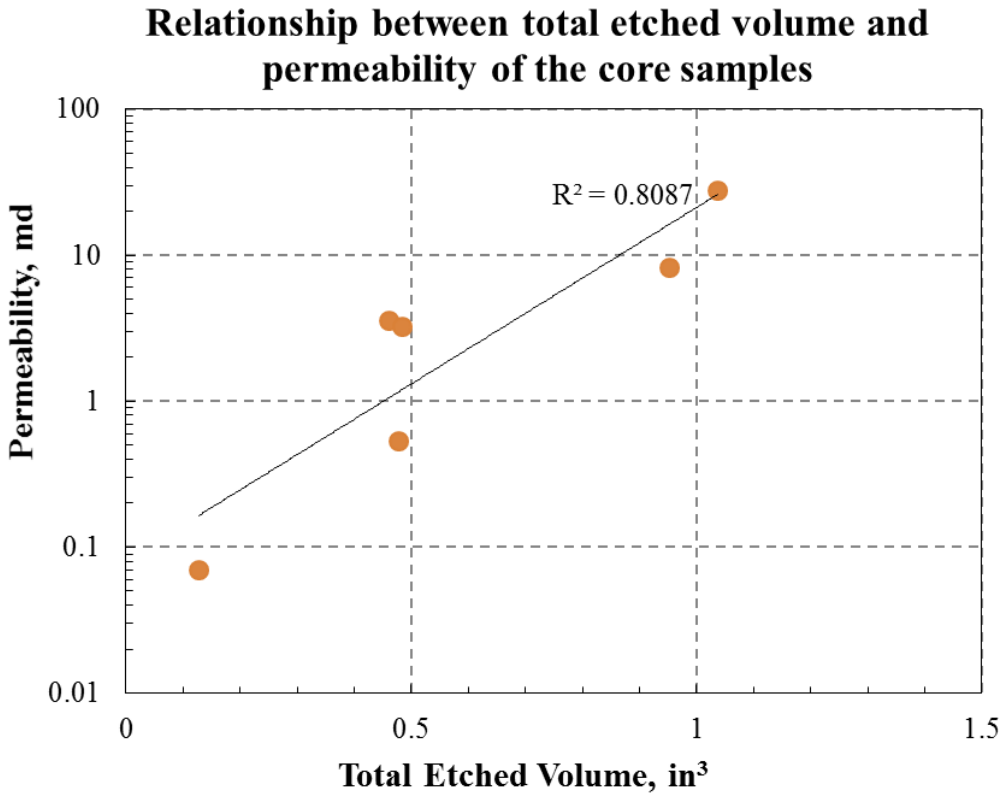

Figure 12. The relationship between the total etched volume of the rock and the permeability of the core samples

The fracture surface profiles for the cores treated by acid during 20 minutes are shown in **Figure 13 - Figure 17.** The 3D images indicate the difference in fracture surface topography generated by acid etching. The most profound etching was observed for the core KM 6831. This core sample had the highest permeability among all the samples. The peaks seen on the lower picture were generated due to defocusing of laser during scanning of the rough surface and should not be considered for the analysis.

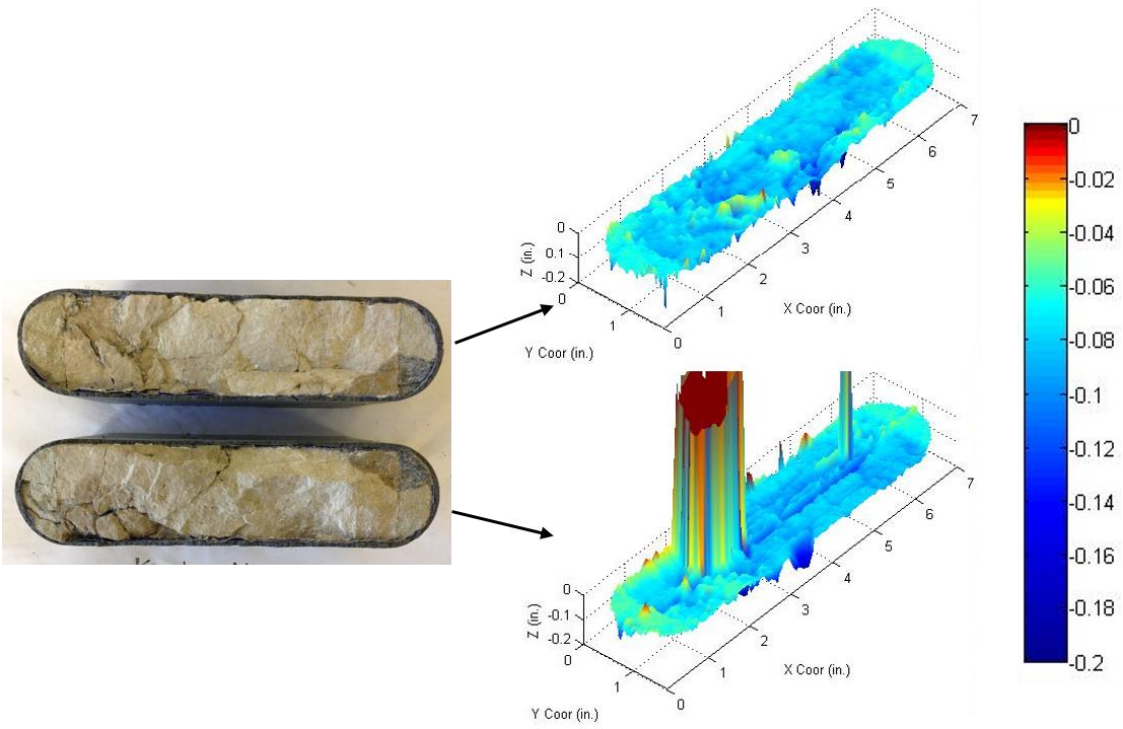

Figure 13. Difference in surface profile created by acid etching of core KM 6831

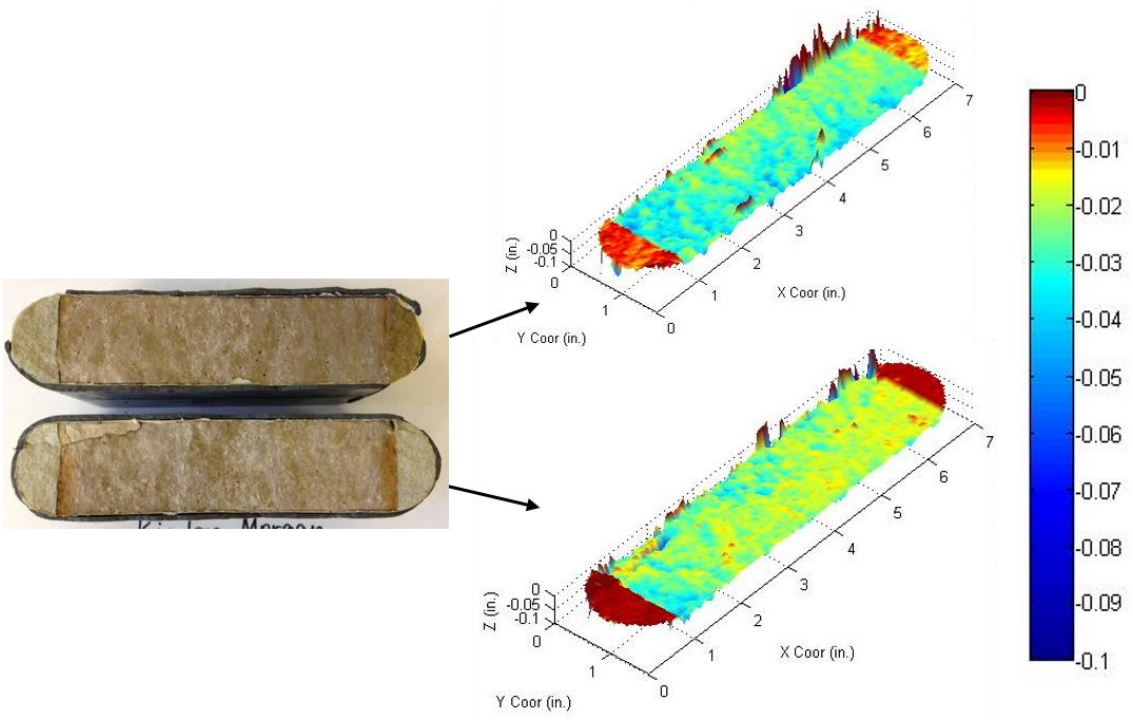

Figure 14. Difference in surface profile created by acid etching of core KM 6847

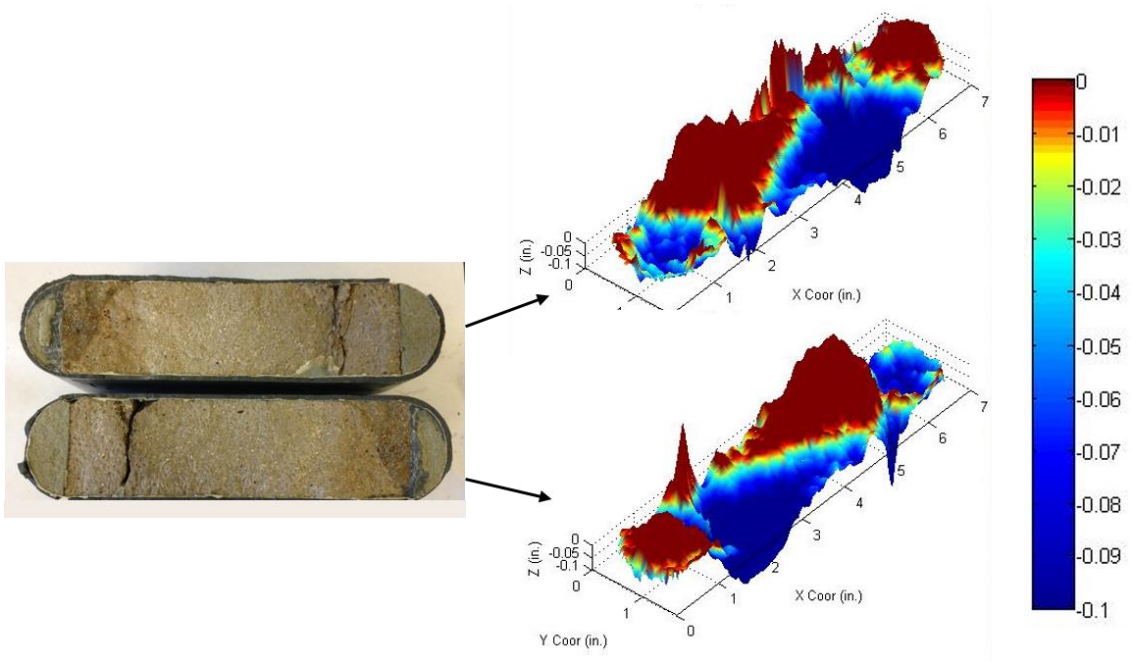

Figure 15. Difference in surface profile created by acid etching of core KM 6891

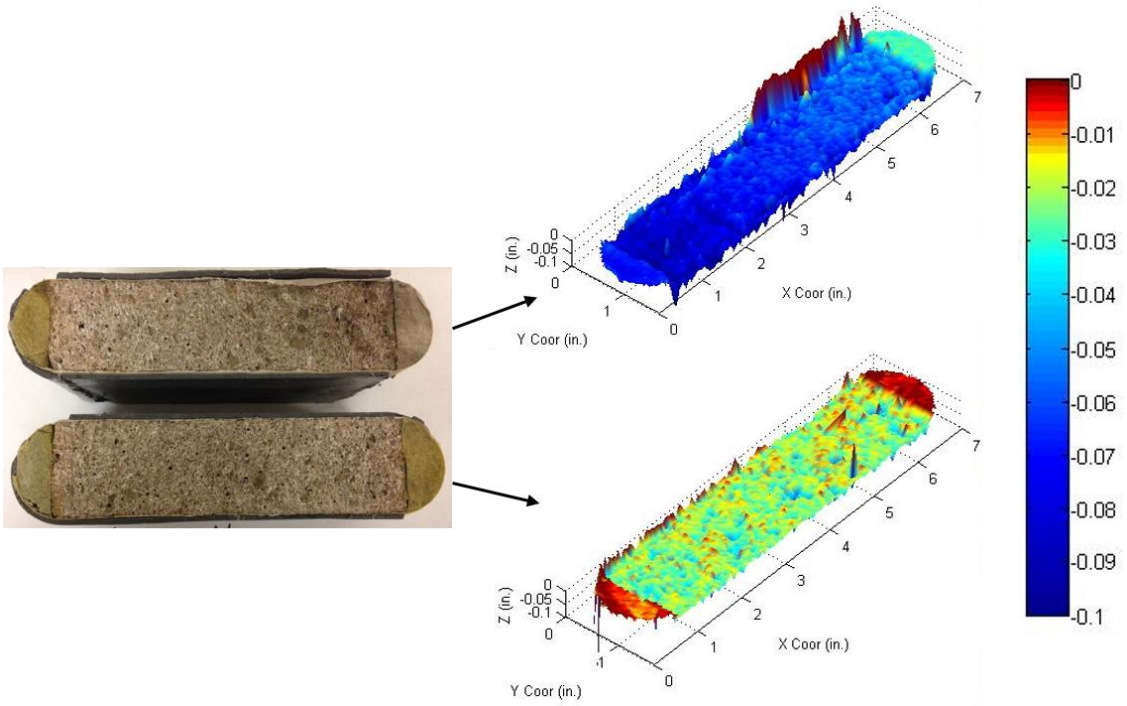

Figure 16. Difference in surface profile created by acid etching of core KM 6898

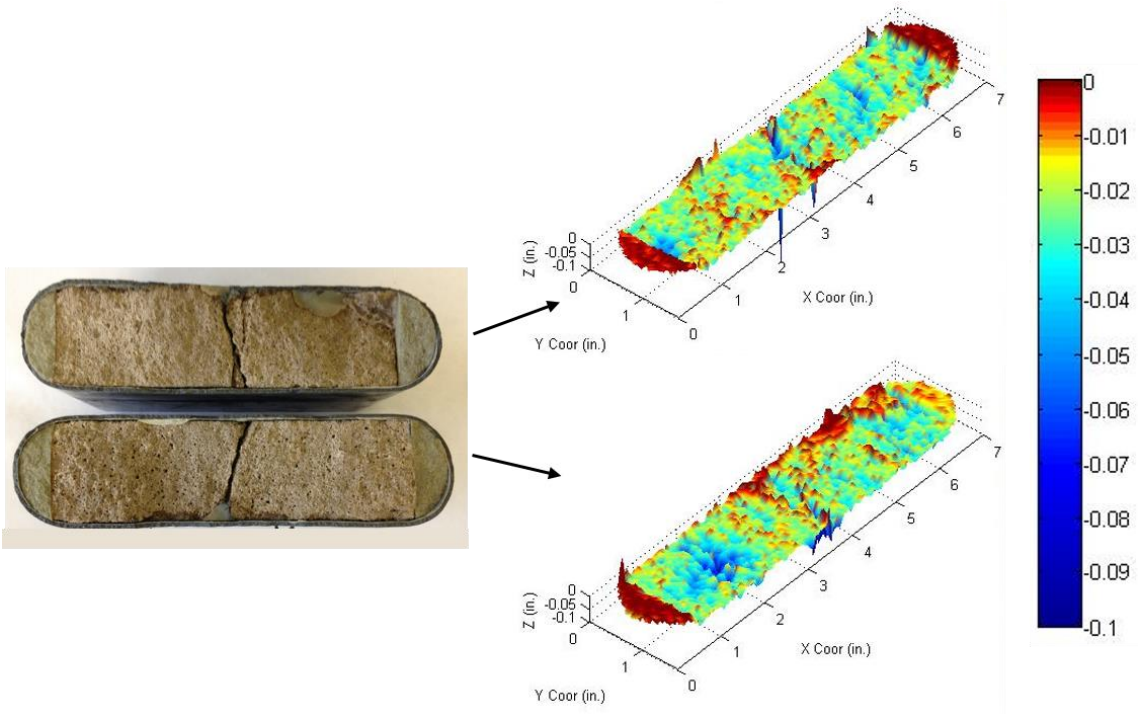

Figure 17. Difference in surface profile created by acid etching of core KM 6901

3.5 Acid Fracture Conductivity Results

Acid fracture conductivity was measured for all the six cores after the acid etching tests. The conductivity was measured under eight closure stress values: 500, 1500, 2000, 2500, 3000, 3500, and 4000 psi. The highest closure stress during the experiment represents the formation closure stress at the field. The conductivity measured at 4000 psi load represents a field case of the retained acid fracture conductivity after the injection of acid is stopped and the formation closure stress is applied to the created fracture. The acid fracture conductivity as a function of closure stress is shown in **Figure 18** for all the cores.

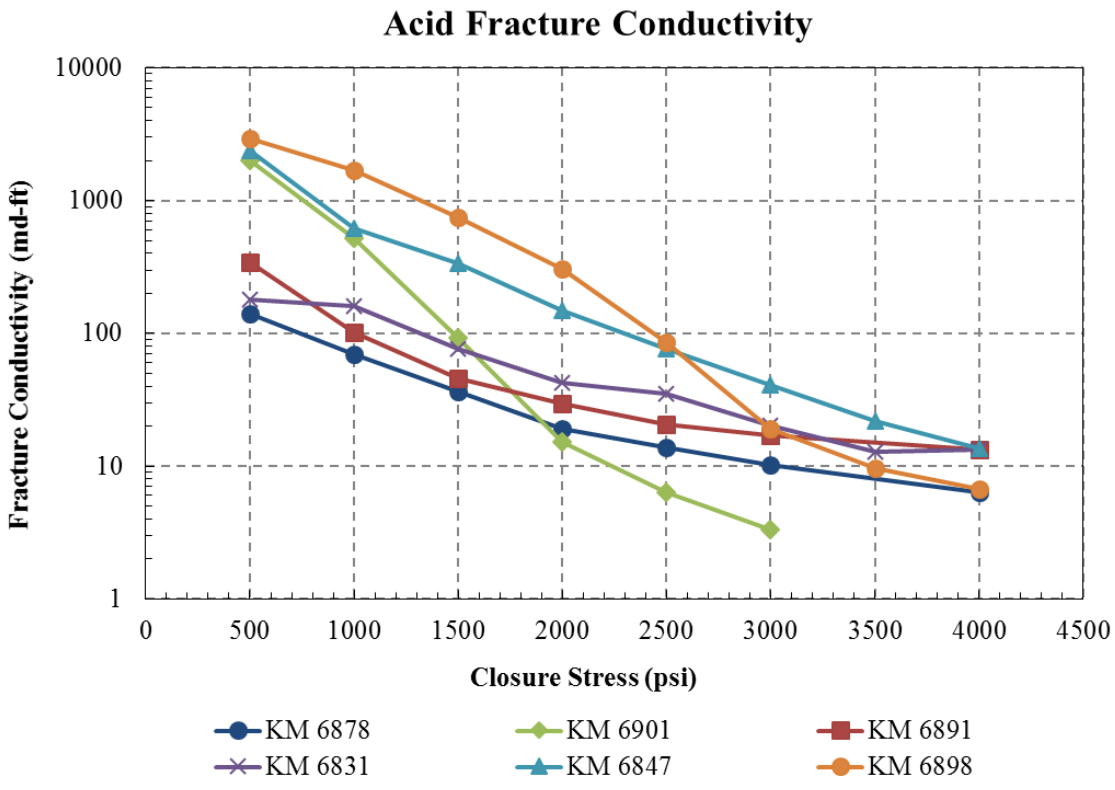

Figure 18. Acid fracture conductivity values for tested cores

The analysis of the conductivity results indicated that the final values of acid fracture conductivity at 4000 psi closure stress laid in the range of 6.4 to 13.5 md-ft. The exception was the core KM 6901, which had the fastest rate of conductivity decline with the conductivity value of 3.4 md-ft measured at 3000 psi closure stress and a complete fracture closure at 4000 psi. Such a unique behavior of this core may be attributed to the etching pattern, where both sides of the core had a similar degree of etching, while for the rest of the cores one of the sides was etched to a greater degree than the other one. Also, the presence of a wide fracture penetrating into the both side of the core could make the fracture faces less resistant to the applied stress and lead to rock crushing near the fractures. The conductivity results for KM 6901 will be eliminated for the future analysis.

As can be seen from the conductivity plot, the tested cores can be grouped into two categories. The first category comprise the core samples KM 6831, KM 6878, and KM 6891, which have a lower rate of conductivity decline with increasing closure stress. The decline rate is similar for all the three samples. The conductivity values for cores KM 6831 and KM 6891 with 20 minutes contact time during acid treatment are higher at all closure stresses than for KM 6878 with 10 minutes contact time of. Thus, the increase of contact time improved the performance of created acid fracture. In contrast to the samples discussed above, the second category of samples consist of cores KM 6847 and KM 6898, which are characterized with much faster conductivity decline rate. Both of these cores had significantly lower leak-off volumes than samples KM 6891 and KM 6831 from the first category. Acid fracture conductivity of core KM 6847 showed the

best performance among all the cores tested with conductivity values being larger at higher closure stress compared to the other cores. However, the final conductivity for this core was 13.5 md-ft under 4000 psi closure stress, being similar to cores KM 6831 and KM 6891 with a lower decline rate of conductivity. Although, the conductivity for core KM 6898 was the highest among all the cores at lower closure stress, it decreased fast and reached only 6.7 md-ft at the maximum closure stress.

It was observed that the decline rate of fracture conductivity with increasing closure stress correlated with the porosity of core samples. Thus, the cores samples with a lower decline rate had lower porosity, while the samples that showed faster conductivity decline had higher porosity values. The reason for this can be the effect of rock porosity on a formation compressibility under a closure stress. With greater porosity, the potential of rock to be compressed under the stress is higher, which leads to a greater fracture closure and to a faster conductivity decline. In contrast, the rock which has a lower porosity is less compressible, so the conductivity sustains better under the increasing closure stress.

CHAPTER IV

CONCLUSIONS AND RECOMMENDATIONS

The following conclusions can be derived from the experimental results:

1. Selection of the optimum contact time is important to achieve a higher etched volume and a resultant acid fracture conductivity.
2. The decline rate of acid fracture conductivity with increasing closure stress depends on rock porosity. The cores with a lower porosity had a lower conductivity decline rate, while the cores with a higher porosity had much faster conductivity decline.
3. The increase of total etched volume of the rock was observed with increasing permeability of the core samples.
4. Despite a significant variation in cores' porosity and permeability, the final conductivity values under the maximum closure stress laid within a narrow range between 6.4 and 13.5 md-ft.
5. The resultant acid fracture conductivity obtained for all the tested cores showed that acid fracturing stimulation of the Middle Canyon formation may not be effective to achieve a sufficient injectivity of horizontal wells at the field.

The recommendations based on the analysis of experimental results are given below:

1. Additional experiments on the cores with different porosities and permeabilities are required to better understand the effect of these parameters on etching pattern, etched volume and leak-off volume.

2. Measurement of rock mechanical properties, such as rock embedment strength, Young's modulus, and Poisson's ratio is recommended to understand the performance of created acid fracture under closure stress and its ability to retain conductivity.

REFERENCES

Abass, H.H., Al-Mulhem, A.A., Alqam, M.H. et al. 2006. Acid Fracturing or Proppant Fracturing in Carbonate Formation: A Rock Mechanics View. Presented at the SPE Annual Technical Conference and Exhibition, San Antonio, Texas, 24-27 September. SPE-102590-MS. http://dx.doi.org/10.2118/102590-MS.

Anderson, M.S. and Fredrickson, S.E. 1989. Dynamic Etching Tests Aid Fracture-Acidizing Treatment Design. *SPE Prod Eng* **4** (4): 443-449. SPE-16452-PA. http://dx.doi.org/10.2118/16452-PA.

Barron, A.N., Hendrickson, A.R., and Wieland, D.R. 1962. The Effect of Flow on Acid Reactivity in a Carbonate Fracture. *JPT* **14** (4): 409-415. SPE-134-PA. http://dx.doi.org/10.2118/134-PA.

Bartko, K.M., Conway, M.W., Krawietz, T.E. et al. 1992. Field and Laboratory Experience in Closed Fracture Acidizing the Lisburne Field, Prudhoe Bay, Alaska. Presented at the SPE Annual Technical Conference and Exhibition, Washington, DC, 4-7 October. SPE-24855-MS. http://dx.doi.org/10.2118/24855-MS.

Beg, M.S., Kunak, A.O., Gong, M. et al. 1998. A Systematic Experimental Study of Acid Fracture Conductivity. *SPE Prod & Fac* **13** (4): 267-271. SPE-52402-PA. http://dx.doi.org/10.2118/52402-PA.

Broaddus, G.C., Knox, J.A., and Fredrickson, S.E. 1968. Dynamic Etching Tests and Their Use in Planning Acid Treatments. Presented at the SPE Oklahoma Regional

Meeting, Stillwater, Oklahoma, 25 October. SPE-2362-MS. http://dx.doi.org/10.2118/2362-MS.

de Rozieres, J. 1994. Measuring Diffusion Coefficients in Acid Fracturing Fluids and Their Application to Gelled and Emulsified Acids. Presented at the SPE Annual Technical Conference and Exhibition, New Orleans, Louisiana, 25-28 September. SPE-28552-MS. http://dx.doi.org/10.2118/28552-MS.

Gomaa, A.M. and Nasr-El-Din, H.A. 2009. Acid Fracturing: The Effect of Formation Strength on Fracture Conductivity. Presented at the SPE Hydraulic Fracturing Technology Conference, The Woodlands, Texas, 19-21 January. SPE-119623-MS. http://dx.doi.org/10.2118/119623-MS.

Gong, M., Lacote, S., and Hill, A.D. 1998. A New Model of Acid Fracure Conductivity Based on Deformation of Surface Asperities. Presented at the SPE Formation Damage Control Conference, Lafayette, Louisiana, 18-19 February. SPE-39431-MS. http://dx.doi.org/10.2118/39431-MS.

Melendez, M.G. 2007. The Effects of Acid Contact Time and Rock Surfaces on Acid Fracture Conductivity. Master of Science, Texas A&M University. http://hdl.handle.net /1969.1/ETD-TAMU-1956.

Nierode, D.E. and Kruk, K.F. 1973. An Evaluation of Acid Fluid Loss Additives Retarded Acids, and Acidized Fracture Conductivity. Presented at the Fall Meeting of the Society of Petroleum Engineers of AIME, Las Vegas, Nevada, 30 September-3 October. SPE-4549-MS. http://dx.doi.org/10.2118/4549-MS.

Pournik, M., Gomaa, A.M., and Nasr-El-Din, H.A. 2010. Influence of Acid-Fracture Fluid Properties on Acid-Etched Surfaces and Resulting Fracture Conductivity. Presented at the SPE International Symposium and Exhibiton on Formation Damage Control, Lafayette, Louisiana, 10-12 February. SPE-128070-MS. http://dx.doi.org/10.2118/128070-MS.

Van Domelen, M.S. 1992. Optimizing Fracture Acidizing Treatment Design by Integrating Core Testing, Field Testing, and Computer Simulation. Presented at the International Meeting on Petroleum Engineering, Beijing, China, 24-27 March. SPE-22393-MS. http://dx.doi.org/10.2118/22393-MS.

Van Domelen, M.S., Gdanski, R.D., and Finley, D.B. 1994. The Application of Core and Well Testing to Fracture Acidizing Treatment Design: A Case Study. Presented at the European Production Operations Conference and Exhibition, Aberdeen, United Kingdom, 15-17 March. SPE-27621-MS. http://dx.doi.org/10.2118/27621-MS.